Journal of the European Ceramic Society 20 (2000) 1077–1084

Effect of ceria content on the sintering of ZrO_2 based ceramics synthesized from a polymeric precursor

Antonio. L Quinelato[a], Elson Longo[b], Leinig A. Perazolli[c], José A. Varela[c,*]

[a]*Comissão Nacional de Energia Nuclear, Poços de Caldas, Brazil*
[b]*Departamento de Química, Universidade Federal de São Carlos, Brazil*
[c]*Instituto, de Química, Universidade Estadual Paulista, São Paulo, Brazil*

Received 13 May 1999; received in revised form 6 September 1999; accepted 8 October 1999

Abstract

Zirconia-ceria powders with ceria concentration varying from 0 to 12 mol% were synthesized using a polymeric precursor route based on the Pechini process. Powder characteristics were evaluated with regard to the crystallite size, BET surface area, phase distribution, nitrogen adsorption/desorption behavior, and agglomeration state. Sintering was studied considering the shrinkage rate, densification, grain size, and phase evolution. It was demonstrated that the synthesis method is effective to prepare nanosized powders of tetragonal zirconia single-phase. Sinterability mainly depended on the agglomeration state of powders and the monoclinic phase content. Fully tetragonal zirconia ceramic, with grain size of 2.4 μm, was obtained after addition of at least 9 mol% ceria and sintering at 1500°C for 4 h.

Keywords: CeO_2; Microstructure-final; Powders-chemical preparation; Precursors-organic; Sintering; ZrO_2

1. Introduction

Zirconia is normally monoclinic (*m*) at room temperature, but undergoes a reversible difflusionless martensitic phase transformation at about 1200°C to a tetragonal(*t*) structure.[1,2] The transformation leads to the shape and volume change, so that severe cracking often appears if ceramics are cycled through the transition temperature, which renders the material useless for structural applications. Thus, spontaneous *t*- to *m*-transformation during cooling from the fabrication or service temperature must be avoided. Furthermore the *t*- phase can be retained below the standard transformation temperature and in some cases until below room temperature. The addition of ceria for making a solid solution with zirconia can result in a single-phase *t*-structure[3–7] denominated tetragonal zirconia polycrystals (TZP). The phase relationship[8,9] shows an extensive solid-solution region in which the *t*- phase is stable at room temperature. Ce-TZP possesses a high fracture toughness and thermal stability, considered to be caused by stress-induced transformation from the *t*- to *m*-phase.[10–12] This transformation renders the toughening mechanism effective, and again, spontaneous transformation must be avoided.

Strong evidences support the particle size effect on the *t*-phase stabilization at room temperature. Holmes et al.,[13] determined by using heat of immersion that the surface free energy of *t*-zirconia is smaller than that of *m*-structure. This fact was considered as the stabilizing factor for the occurrence of the *t*-form in small particles. Garvie[14] also explained this particle effect in terms of the lower surface energy of the *t*-phase compensating for the differences in chemical free energy. Thus if a critical particle size is exceeded, the *t*-phase is transformed to the *m*-phase, but at any given temperature, this size is strongly dependent on any hydrostatic and/or non-hydrostatic stress present. Shi et al.[15] showed that the doping of stabilizer oxides (MgO, $YO_{1,5}$, and CeO_2) reduces the particle size by the decrease of the surface energy, but the size-reducing effect is different for each oxide. That is, the decrease of size with the increase of dopant level is distinguished and depends on the dopant. The influence of the particle size on the *t*-phase stability has also been reported by some other investigators,[4,16,17]

* Corresponding author. Tel.: +55-16-222-0015; fax: +55-16-222-7932.
E-mail address: varela@iq.unesp.br (J.A. Varela).

0955-2219/00/$ - see front matter
PII: S0955-2219(99)00269-1

by using different methods of synthesis of zirconia-based ceramic powders.

The grain size of the sintered ceramic must also be kept below a critical value to retain the *t*-phase at room temperature. This value depends, among other factors, on the concentration and type of oxide used to stabilize the *t*-phase. Ceria reduce the extent of grain growth and thus decrease the grain size of the sintered ceramics,[18] and for any ceria content the fraction of the *m*-phase increase with the grain growth. The grain size is also affected by characteristics of the starting powder, which differs depending on the synthesis methods and conditions used. These characteristics include purity, homogeneity, particle shape and size, particle size distribution, presence of agglomerates, etc.[19]

A wet-chemical method using polymeric precursor based on the Pechini process,[20] has been used to synthesize various ceramic powders.[21–26] The method offers several advantages for processing ceramic powders such as direct and precise control of stoichiometry, uniform mixing of multicomponents on a molecular scale, and homogeneity. The method was applied to synthesize zirconia-ceria[7] showing to be effective to prepare zirconia with a tetragonal structure.

The objective of the present study is to investigate the effect of the CeO_2 content on the zirconia-ceria powder characteristics, using polymeric precursor based on the Pechini process as synthesis method, and also to evaluate the sintering behavior and microstructures of sintered ceramic.

2. Experimental procedure

2.1. Synthesis of ZrO_2–CeO_2 powders

Zirconium(IV) oxide chloride, $ZrOC1_2.8H_2O$ (Merck, Darmstadt, Germany) was first dissolved into distilled water. Zirconium hydroxide was precipitated from this solution by amnionium hydroxide addition until pH = 8.0. The solution thus obtained was then filtered. The liquid phase was discarded and the zirconium hydroxide was washed with distilled water until complete elimination of chlorine ions in the liquid phase. The zirconium hydroxide was then dissolved with nitric acid for preparation of zirconium nitrate solution.

Cerium hydroxide (Nuclemon, São Paulo, Brazil) was dissolved in concentrated nitric acid at 80°C, for preparation of cerium nitrate solution.

Zirconium and cerium nitrate solutions were mixed in a beaker, considering the desired stoichiometry of the metal oxides in the final ceramic powder. On stirring, the mixture was heated to about 100°C. Citric acid (CA) was then added to chelate metal cations. at the CA: total oxides molar ratio (CA:TO) of 4:1. Total oxides denote the sum of ZrO_2 plus CeO_2 in the final ceramic powder. After 15 min ethylene glycol (EG) was added into solution at a CA:EG molar ratio of 1:5. The colorless solution thus obtained, was then heated up to 140°C, and kept under stirring to promote the esterification and polymerization reactions. After nitrous oxides and water elimination, a clear resin was obtained. The polymeric resin was charred at 250°C to remove organic substances. The black powder thus produced was ball milled and calcined for 2 h in a crucible at 600°C, to obtain the ceramic powder. The CeO_2 contents were 0, 2, 4, 7, 8, 9 and 12 mol%.

The procedures of powder synthesis and sintering are outlined in the flow chart in Fig. 1.

2.2. Sintering

The powders were compacted using direct uniaxial pressing into cylindrical pellets with 9 mm diameter, under a pressure to give the green density about 37% of theoretical value. These samples were sintered in a dilatometer furnace (Nestzch model 402 E), with a constant heating rate of 10°C/min and in an electrical box furnace at 1500°C for 4 h in atmospheric air. The densities after sintering were measured by weighing the samples and determining their volume by the Archimedes method. The theoretical densities were calculated from lattice parameter measurements by XRD.

2.3. Characterization

The existing phases in the ceramic powders and sintered bodies were investigated by X-ray diffraction-XRD (Siemens diffractometer, model D-5000, with CuK_α radiation and graphite monochromator).

For the monoclinic-tetragonal ZrO_2 system, the fraction of monoclinic phase was calculated using the integrated intensity ratio of the diffraction peaks.[27]

The mean crystallite sizes of the calcined powder were calculated using the X-ray line broadening method, through the Scherrer relationship.[28,29] Nitrogen adsorption/desorption on the powder surface at 77 K (Micromeritics, ASAP 2000) was used to verify the hysteresis occurrence and to measure the specific surface area by applying the BET method.[28] Samples were outgassed at 250°C for 2 h prior to each analysis, to remove eventual physisorbed species from the powder surface.

The powder morphology was observed using transmission electron microscopy (Philips-CM200 microscope). Powders were dispersed in ethyl alcohol using an ultrasonic treatment. A drop of the resulting suspension was put on a microscopic grid previously covered with a polymer and carbon film. The microstructures of the surfaces of as-sintered samples were analyzed using scanning electron microscopy (TOPCOM-300 microscope). The average grain sizes were estimated by the linear intercept method.

3. Results and discussion

3.1. Powder synthesis and morphology

The XRD patterns of the powders with different CeO_2 content (Fig. 2) show that the monoclinic phase occurred only in pure zirconia powder, which presented 21.7% of the *m*-phase and 78.3% of the *t*-phase. For the other powders, a well-crystallized tetragonal zirconia single-phase were obtained. The CeO_2 content affected both crystallite size and surface area of the powders, as observed in Fig. 3. As observed in this figure, the crystallite size decreases with the increase of the CeO_2 content, i.e. crystallite growth of zirconia is inhibited by the ceria doping in zirconia. The mean crystallite size ranges from 7 to 21 nm showing that the method is effective for synthesis of nanosized powders. Surface areas decreased with a decrease of the CeO_2 content because of the crystallite coarsening. Under the experimental conditions, pure zirconia shows the largest mean crystallite size of 21 nm and the size is reduced to about 7 nm when 12 mol% CeO_2 is used. This suggests that increasing ceria content reduces the surface free energy of zirconia particles and so decreases the crystallise size, which is accompanied by a more effective tetragonal phase stabilization. It is important to notice that the powder containing 2 mol% CeO_2 presented mean crystallite size of about 16 nm and tetragonal zirconia single-phase. This indicates that under the experimental conditions used in the zirconia–ceria synthesis, the critical

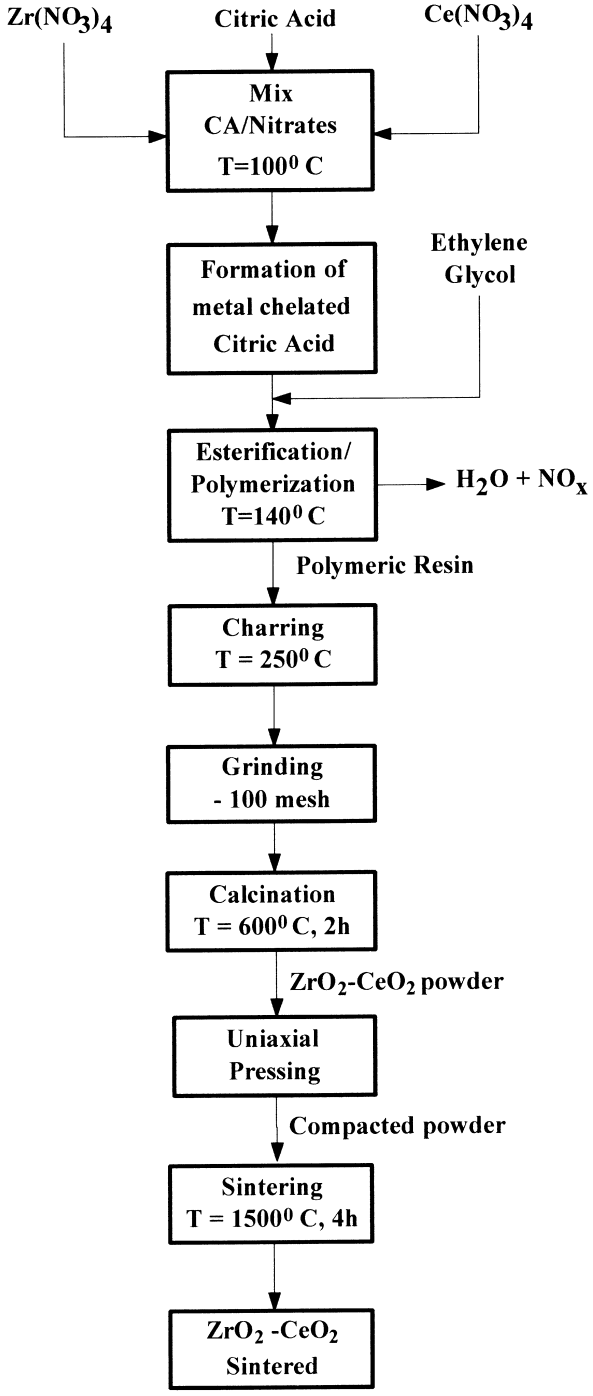

Fig. 1. Flow chart of polymeric precursor synthesis and preparation of ZrO_2–CeO_2 sintered bodies.

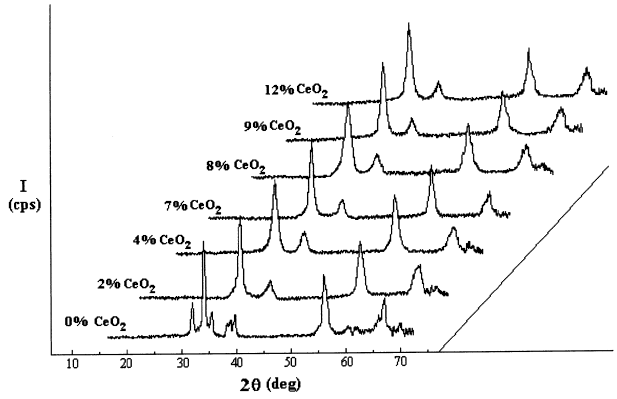

Fig. 2. X-ray diffraction patterns of ZrO_2–CeO_2 powders calcined at 600°C for 2 h.

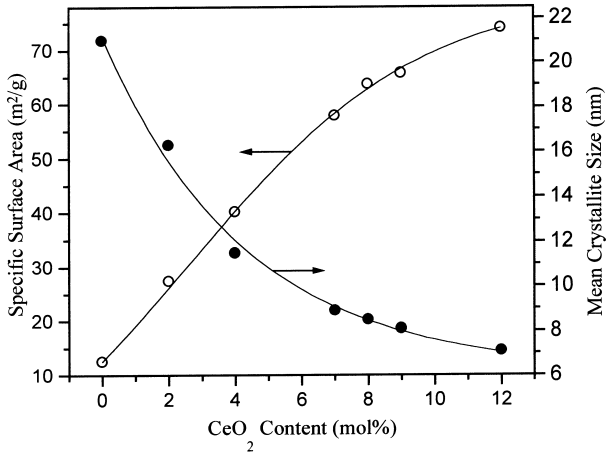

Fig. 3. Mean crystallite size and BET surface area of ZrO_2–CeO_2 powders as a function of CeO_2 content.

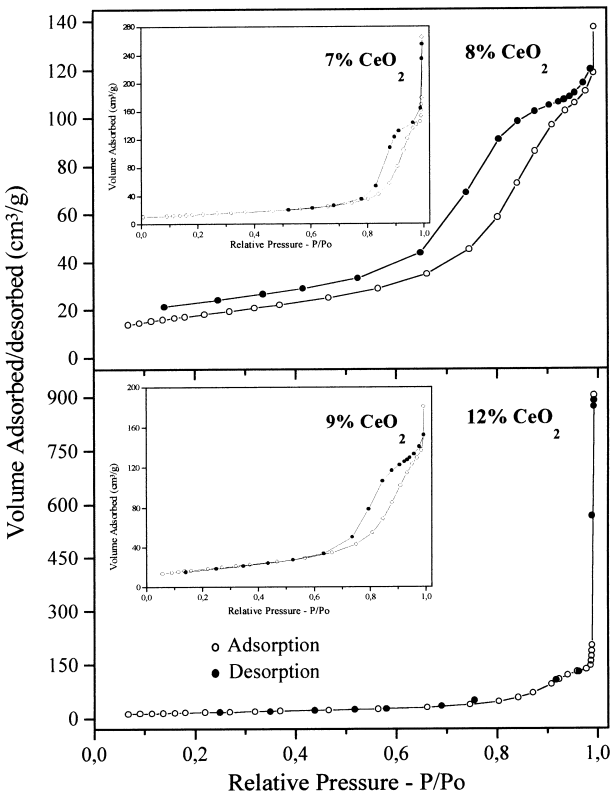

Fig. 4. Nitrogen adsorption/desorption curves for the ZrO_2–CeO_2 powders.

crystallite size for tetragonal-to-monoclinic transformation is larger than 16 nm.

The nitrogen adsorption/desorption isotherms for the powders synthesized using CeO_2 content of 7, 8, 9 and 12 mol% are shown in Fig. 4. For powders containing 7, 8, and 9 mol% CeO_2 the nitrogen adsorption/desorption behavior were similar, showing the occurrence of hysteresis, indicating that capillary condensation in mesopore structures occur.[30] This suggests the presence of aggregates, which are understood here, as being strong and hard partially sintered or cemented groups of particles. For powder containing 12 mol% CeO_2 the isotherms were coincident, that is, no hysteresis was observed, suggesting that the powder be not aggregated. However, this powder showed a direct evidence of some degree of agglomeration, as seen in the TEM micrograph of Fig. 5a. Agglomerates are also present in the powder containing 9 mol% CeO_2, as showed in Fig. 5b. However, the agglomerates in powder containing 12 mol% CeO_2 are less dense, i.e. more transparent to electrons than that containing 9 mol% CeO_2, suggesting soft agglomerates with particles connected by Van der Walls forces. All dry, fine particles can be expected to contain soft agglomerates.

3.2. Sintering behavior and phase stability

The linear shrinkage rate of powder compacts, sintered in a dilatometer with a constant heating rate of

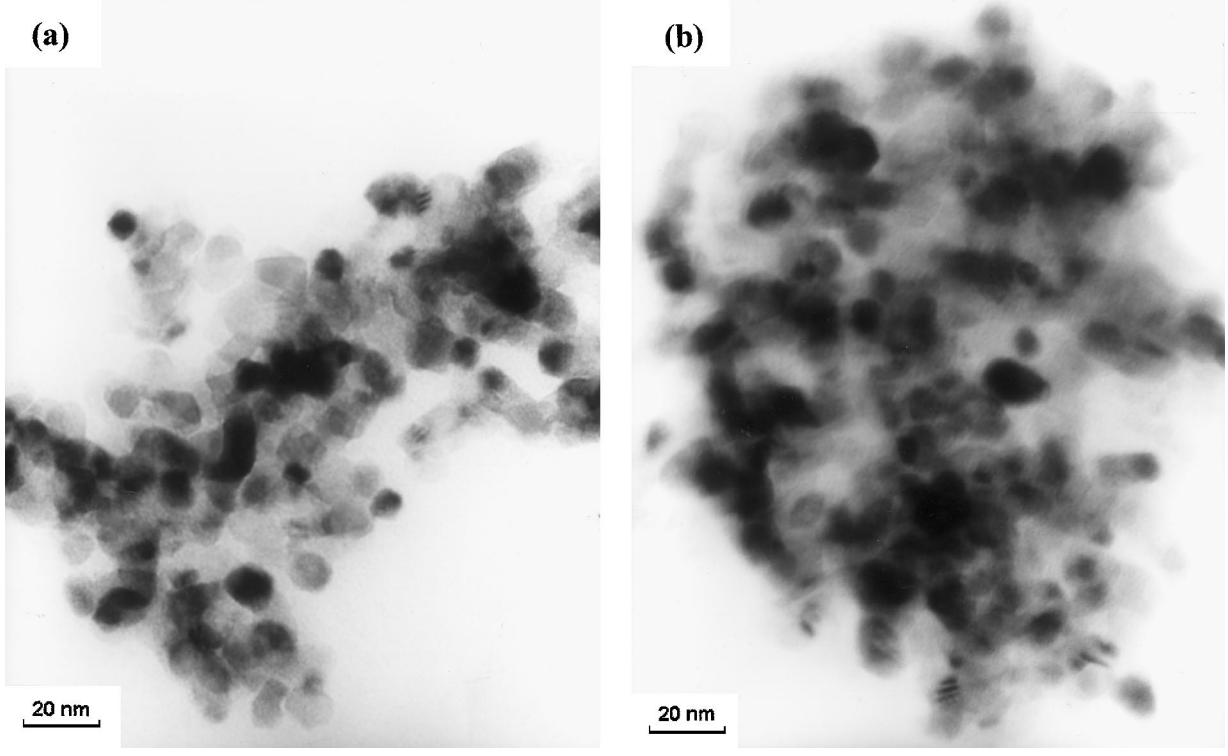

Fig. 5. TEM micrographs of the calcined powders: (a) 12 mol% CeO_2, and (b) 9 mol% CeO_2.

10°C/min is illustrated in the curves of Fig. 6. The curves for powder compacts containing 7, 8 and 9 mol% CeO_2 presented two peaks of the shrinkage rate. This behavior suggests again that aggregates are present. Elimination of the intra-aggregate pores during sintering corresponds to the lower-temperature peak. The higher-temperature peak is connected to the inter-aggregate pore elimination.[31] The temperatures at which both peaks occur decrease with the increase of the CeO_2 content. Finer powders with higher surface areas are obtained with the increase of CeO_2 content, which tends to sinter at lower temperatures. It can also be observed that the intensity of the lower-temperature peak decreases with increasing CeO_2 content and disappears with 12 mol% CeO_2 (for this concentration there is only one peak). This suggests that increasing CeO_2 content, the concentration of intra-aggregate pores are decreased, meaning a reduction of the aggregates content, up to the disappearance for the powder containing 12 mol% CeO_2. These results corroborate the observation based on data from studies of nitrogen adsorption/desorption and TEM.

The X-ray diffraction patterns for samples sintered at 1500°C for 4 h are shown in Fig. 7. The fraction of monoclinic phase in as-sintered ceramics as a function of the CeO_2 content, obtained from these patterns, is represented in Fig. 8a. The monoclinic fraction decreases with increasing CeO_2 content. The samples containing 7 and 8 mol% CeO_2 presented 100 and 74.6% of monoclinic phase respectively, while the samples containing 9 and 12 mol% CeO_2 presented only tetragonal zirconia single-phase. Thus, 9 mol% CeO_2 is sufficient to obtain a fully tetragonal phase.

The average grain size as a function of the CeO_2 content is represented in Fig. 8b. The grain size decreases from 3.3 to 2.2 μm with increasing CeO_2 content from 7 to 12 mol%. Thus, increasing ceria content inhibits grain growth and decreases the amount of monoclinic phase in the sintered ceramics. Moreover, increasing CeO_2 content the crystallite size decreases, which probably also contribute for decrease in grain sizes of the

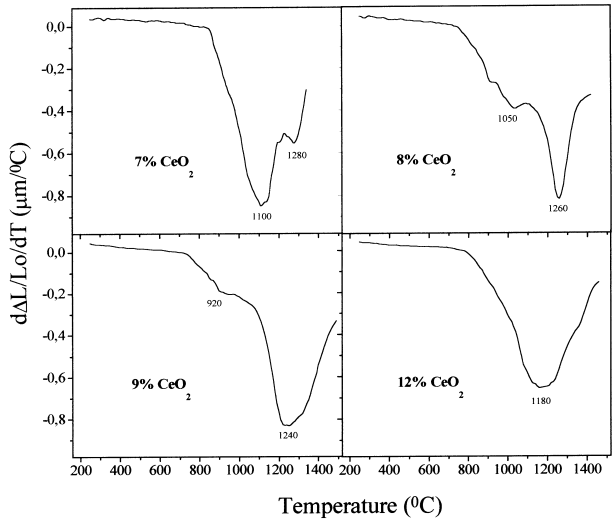

Fig. 6. Linear shrinkage rate as a function of temperature of ZrO_2–CeO_2 ceramics with different ceria concentration.

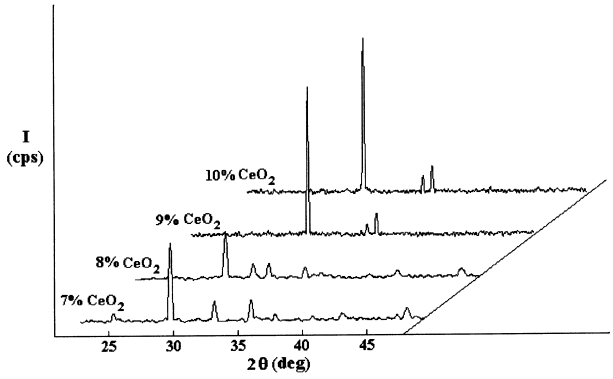

Fig. 7. X-ray diffraction patterns of ZrO_2–CeO_2 samples sintered at 1500°C for 4 h.

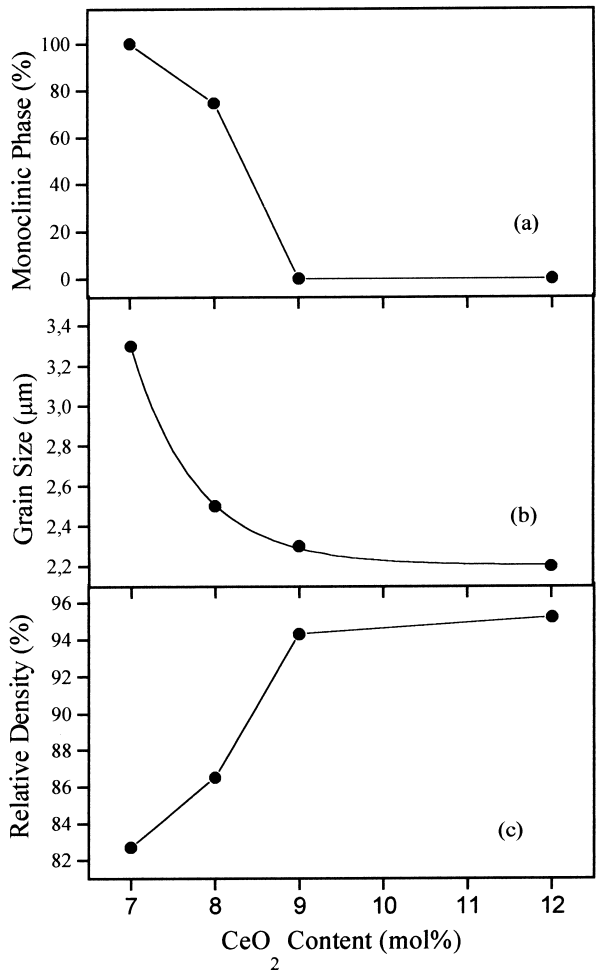

Fig. 8. (a) Monoclinic phase content, (b) grain size, and (c) relative density, as a function of CeO_2 content, of the samples sintered at 1500°C for 4 h.

sintered material. The critical grain size for retention of the tetragonal phase was about 2.4 μm, considering the powder containing 9 mol% CeO_2.

The relative densities as a function of the CeO_2 content are represented in Fig. 8c. Increasing CeO_2 content favors the densification as shown in this figure. The density increases from 86 to 97% of theoretical densities with increasing CeO_2 content from 7 to 12 mol%. The decrease in relative density with decreasing CeO_2 content can be attributed to the formation of microcracking associated with the tetragonal-to-monoclinic phase transformation. However, microcracking is not the only factor affecting the decrease of the density after sintering. For instance, the samples containing 9 and 12 mol% CeO_2 composed by tetragonal single-phase, presented different relative densities of 95 and 97% of theoretical, respectively. The characteristics of the powder compact determine in turn the sintering behavior. Complete densification is possible only for a high degree of homogeneity of the microstructure in the compact i.e. a high degree of homogeneity of the packing in the green compact. To obtain homogeneous packing, the powder should have a small crystallite size and should be unagglomerated. However, agglomerates are present especially in submicrometer powder synthesized by wet-chemical routes. But, a powder consisting of soft agglomerates, which can be easily destroyed during compaction at relatively low pressures, can form inter and intra-agglomerate pores of same size with a narrow pore size distribution. In this case, the driving force for sintering is also uniform across the whole body. The resultant densification is high. A powder consisting of

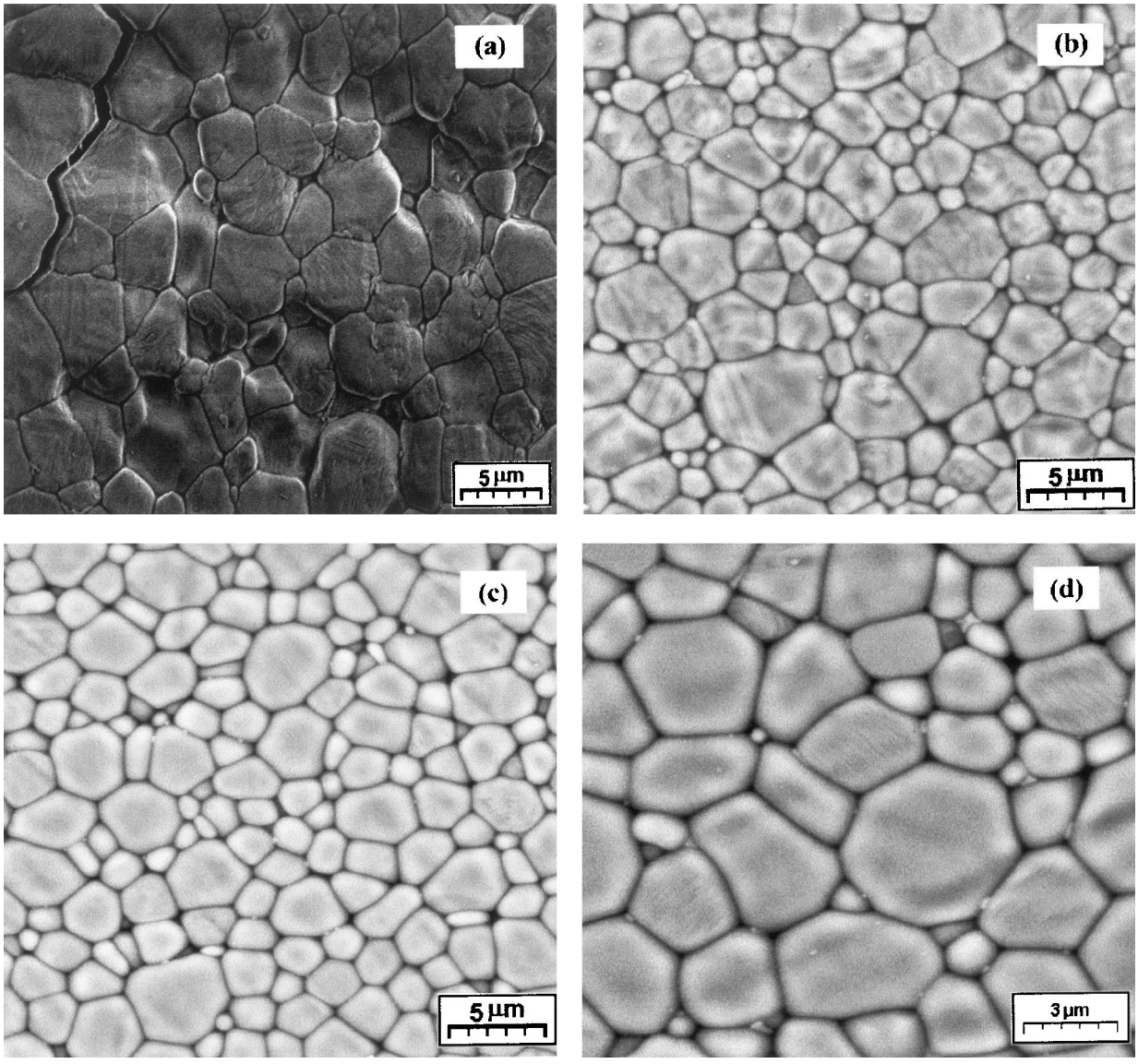

Fig. 9. SEM micrographs showing the microstructure Of ZrO_2–CeO_2 sintered at 1500°C for 4 h, containing: (a) 7 mol% CeO_2; (b) 8 mol% CeO_2; (C) 9 mol% CeO_2; (d) 12 mol% CeO_2.

hard agglomerates (aggregates) cannot be compacted to such a homogeneous pore size distribution.[32] In this case, the intra-agglomerate porosity is removed very effectively at low temperatures but the disappearance of inter-agglomerate porosity at higher temperatures is much less effective. The resultant densification of the whole body can be poor. Thus, considering that the powders synthesized at different CeO_2 content were compacted to the same green densities (37% of theoretical), can suggest that the microstructure in the compact also affected the density of sintered ZrO_2–CeO_2. Therefore, the decrease of the sintered density is also associated to the increase of crystallite size and presence of aggregates, which are favored by decreasing CeO_2 content. Although the densities after sintering have been relatively poor, higher densities could be obtained by improving the green compaction of the powders.

The microstructure of as-sintered ZrO_2–CeO_2 obtained by the SEM is represented in Fig. 9. For the sample containing 7 mol% CeO_2 intergranular cracking is visible, due to effective tetragonal-to-monoclinic transformation during cooling process after sintering, as indicated in Fig. 9a. For concentrations of 9 and 12 mol% of ceria the sintered samples showed no crack formation since only tetragonal phase was found in those samples (Fig. 9c and d).

4. Conclusions

Zirconia-ceria powders synthesized by a polymeric precursor method based on the Pechini process presented tetragonal zirconia single-phase, even when a reduced content of 2 mol% CeO_2 is used, due to presence of small crystallites with sizes of 16 nm.

The ceria content affected the powder characteristics. Increasing ceria content produced finer powders with higher specific surface area. Powder containing 12 mol% CeO_2 presented crystallite size of 7 nm and surface area of 74 m^2/g. It was also demonstrated that the aggregate content decreases with increasing ceria content. Not aggregated powder was obtained for ZrO_2–12 mol% CeO_2.

The different powder characteristics obviously affected the sintering behavior and the characteristics of the sintered ceramic. To produce ZrO_2–CeO_2 ceramic with single-phase tetragonal zirconia 9 mol% CeO_2 was necessary. The critical grain size for retention of the tetragonal phase with this CeO_2 content was 2.4 μm, under the experimental conditions used.

Densities as high as 97% of theoretical value were achieved for ZrO_2–CeO_2 ceramics after sintering at 1500°C for 4 h. This value can be improved by starting with higher compact green densities.

Acknowledgements

The authors acknowledge CNEN, FINEP, CNPq and FAPESP for financial support of this work.

References

1. Subbarao, E. C., Zirconia — an overview. In *Advances in Ceramics*, ed. A. H. Heuer and L. W. Hobbs. Science and Technology of irconia, The American Ceramic Society, Columbus, 1981, pp. 1–24.
2. Stevens, R., Zirconia and zirconia ceramics. In: *Magnesium Elektron Publication No 113*, 1986, pp. 1–52.
3. Li, P., Chen, I.-W. and Hahn, J. E. P., Effect of dopants on zirconia stabilization — an X-ray absorption study: tetravalent dopants. *J. Am. Ceram. Soc.*, 1994, **77**(5), 1281–1288.
4. Duh, L.-G., Dai, H.-T. and Hsu, W.-Y., Synthesis and sintering behaviour in CeO_2–ZrO_2 ceramics. *J. Mater. Sci.*, 1988, **23**, 2786–2791.
5. Tsukuma, K., Mechanical properties and thermal stability of CeO_2 containing tetragonal zirconia polycrystals. *Am. Ceram. Soc. Bull*, 1986, **65**(10), 1386–1389.
6. Ali M. E.-S., Houte, S.-E. and Sorensen, O. T., Properties of ceria doped tetragonal zirconia ceramics prepared by coprecipitation technique. In *Proceedings of the Riso International Symposium on Metallurgy and Materials Science, Structural Ceramics Processing, Microstructure and Properties*. Riso Nati. Lab., Riso Library, Roskilde, Denmark, 1990, pp. 269–76.
7. Yashima, M., Ohtake, K., Kakihana, M. and Yoshimura, M., Synthesis of metastable tetragonal (t') zirconia — ceria solid solutions by the polymerized complex method. *J. Am. Ceram. Soc.*, 1994, **77**(10), 2773–2776.
8. Tani, E., Yoshimura, M. and Somiya, S., Revised phase diagram of the system ZrO_2–CeO_2 below 1400°C. *J. Am. Ceram. Soc.*, 1983, **66**(7), 506–510.
9. Yashima, M., Takashima, H., Kakihana, M. and Yoshimura, M., Low-temperature phase equilibria by flux method and metastable-stable phase diagram in the ZrO_2–CeO_2 system. *J. Am. Ceram. Soc.*, 1994, **77**(7), 1869–1874.
10. Tsukuma, K., Mechanical properties and thermal stability of CeO_2 containing tetragonal zirconia polycrystals. *Am. Ceram. Soc. Bull*, 1986, **65**(10), 1386–1389.
11. Tsukuma, K. and Shimada, M., Strength, fracture toughness and vickers hardness of CeO_2-stabilized tetragonal ZrO_2 polycrystals (Ce-TZP). *J. Mater. Sci.*, 1985, **20**, 1178–1184.
12. Sato, T. and Shimada, M., Transformation of ceria-doped tetragonal zirconia polycrystals by annealing in water. *Am. Ceram. Soc. Bull*, 1985, **64**(10), 1382–1384.
13. Holmes, H. F., Fuller Jr., E. L. and Gammage, R. B., Heats of immersion in the zirconium oxide-water system. *J. Phys. Chem.*, 1972, **76**(10), 1497–1502.
14. Garvie, R. C., Stabilization of the tetragonal structure in the zirconia microcrystals. *J. Phys. Chem.*, 1978, **82**(2), 218–224.
15. Shi J. L., Lin, Z. X. and Yen, T. S., Effect of dopants on the crystallite growth of superfine zirconia powder. In Technical Report PB95-247789. The Institute of Scientific and Technical Information of China, 1994, pp. 1–6.
16. Hannink, R. H. J., Johnston, K. A., Pascoe, R. T. and Garvie, R. C., Microstructural changes during isothermal aging of a calcia partially stabilized zirconia alloy. In *Advances in Ceramics Vol. 3, Science and Technology of Zirconia*, ed. A. H. Heuer and L. W. Hobbs. The American Ceramic Society, Columbus, OH, 1981, pp. 116–136.

17. Nagarajan, V. S. and Rao, K. J., Evolution of crystallite zirconia structure in heat-treated ceria stabilized zirconia gels. *J. Mater. Res.*, 1991, **6**(12), 2688–2693.
18. Duh, J.-G., Dai, H.-T. and Chiou, B.-S., Sintering, microstructure, hardness, and fracture toughness behavior of Y_2O_3–CeO_2–ZrO_2. *J. Am. Ceram. Soc.*, 1988, **71**(10), 813–819.
19. Dudnik, E. V., Zaitseva, Z. A., Shecchenko, A. V. and Lopato, L. M., Sintering of ultradisperse powders based on zirconium dioxide (review). *Powder Metallurgy and Metal Ceramics*, 1995, **34**(5), 263–271.
20. Pechini M. P., Method of preparing lead and alkaline earth titanates and niobates and coating method using the same to form a capacitor. U.S. Pat. No 3.330.697, July 11, 1967
21. Liu, M. and Wang, D., Preparation of $La_{1-z}Sr_zCo_{1-y}Fe_yO_{3-x}$, thin films, membranes, and coatings on dense and porous substrates. *J. Mater. Res.*, 1995, **10**(12), 3210–3221.
22. Chen, T.-M. and Hu, Y. H., Polymeric precursors for preparation of $Bi_{1,5}Pb_{0,5}Sr_2Ca_2Cu_3O_x$. *J. Sol. State Chem.*, 1992, **97**, 124–130.
23. Chuah, G. K., Jaenicke, S., Chan, K. S., Khor, S. T. and Hill, J. O., A thermal analysis evaluation of the low temperature synthesis of $BaBiO_3$. *J. Thermal Anal.*, 1993, **40**, 1157–1164.
24. Tao, Y. K. and Hor, P. H., Synthesis of $Pb_2Sr_3Pr_5Cu_5Q_x$ and $Pb_2Sr_3PrCuO_d$ by the citrate gel method. *Mater. Chem. Phys*, 1993, **35**, 92–94.
25. Falter, L. M., Payne, D. A., Friedmann, T. A., Wright, W. H. and Ginsberg, D. M., Preparation of ceramic superconductors by the Pechini method. In *British Ceramic Proceedings*, 1989, pp. 261–269
26. Gülgün, M. A., Poppola, O. O. and Kriven, W. M., Chemical synthesis and characterization of calcium aluminate powders. *J. Am. Ceram. Soc.*, 1994, **77**(2), 531–539.
27. Toraya, H., Yoshirnura, M. and Somiya, S., Calibration curve for quantitative analysis of the monoclinic-tetragonal ZrO_2 system by X-ray difiraction. *J. Am. Ceram. Soc.*, 1984, **67**(6), C119–21.
28. Klug, H. and Alexander, L., Crystallite-size determination from line broadening. In *X-ray Diffraction Procedures*. John Willey and Sons, New York, 1954, pp. 491–538
29. Nuffield, E. W., In *X-ray Diffraction Methods*. John Willey and Sons, New York, 1986, pp. 147–148
30. Sing, K. S. W., Reporting physisorption data for gas/solid system with special reference to the determination of surface area and porosity. *Pure & Appl. Chem.*, 1982, **54**(11), 2201–2218.
31. Roosen, A. and Hausner, H., Sintering Kinetics of ZrO_2 Powders. In *Advances in Ceramics, Vol. 12, Science and Technology of Zirconia II,* ed. N. Claussen, M. Raffle, A. H. Heuer. Columbus, American Ceramic Society, OH, 1984, pp. 714–726
32. Roosen, A. and Hausner, H., Techniques for Agglomeration Control During Wet-Chemical Powder Synthesis. *Advanced Ceram. Matter*, 1988, **3**(2), 131–137.